Crystal structure, spectroscopy and ferromagnetostructural behavior of the complex [Cu^{II}(*L*)(Cl)(*L*′)]·H$_2$O (*L* = 2-aminomethylbenzimidazole, *L*′= L-isoleucinate)

Griselda Carpinteyro-López,[a] José Luis Alcántara-Flores, [a] Daniel Ramírez-Rosales, [b] Roberto Escudero,[c] Blanca M. Cabrera-Vivas,[d] Sylvain Bernès,[e] Rafael Zamorano-Ulloa,[b] and Yasmi Reyes-Ortega[a*]

[a] *Centro de Química, Instituto de Ciencias, Universidad Autónoma de Puebla. Edificio 194, Complejo de Ciencias, C. U., San Manuel, Puebla, Pue. 72570, México*
[b] *Departamento de Física, ESFM, IPN, Ave. Instituto Politécnico Nacional S/N, Edif. 9 U.P. Zacatenco, Col. San Pedro Zacatenco, México, D.F. 07738*
[c] *Instituto de Investigaciones en Materiales, Universidad Nacional Autónoma de México. A. Postal 70-360. México, D.F.*
[d] *Facultad de Ciencias Químicas, Universidad Autónoma de Puebla. Edificio 179, C. U., San Manuel. Puebla, Pue. 71570, México*
[e] *Facultad de Ciencias Químicas. UANL, Guerrero y Progreso S/N, Col. Treviño 64570 Monterrey, N, L., México*
E-mail: yreyes@siu.buap.mx

Dedicated to Dr. Rosalinda Contreras Theurel

Abstract

[Cu^{II}(*L*)(Cl)(*L*′)]·H$_2$O **1** (*L* = 2-aminomethylbenzimidazole, *L*′ = L-isoleucinate) compound crystallizes in the orthorhombic space group *P*2$_1$2$_1$2$_1$. A short Cu—O...Cu contact is observed between neighboring molecules in the crystal structure, with a O...Cu separation of 4.214(3) Å. Molecular structure of **1** shows that *L* and *L*′ act as bidentate ligands, forming the base of the square pyramidal geometry environment of the Cu^{II} ion, while the chloro is the fifth apical ligand. UV/VIS spectrum of **1** shows *d-d* transitions with λ_{max} = 603 nm, characteristic of a low symmetry. Far IR spectrum shows ν_{Cu-N} at 493, 404 cm^{-1}, ν_{Cu-O} at 446 cm^{-1}, and at 302 cm^{-1} ν_{Cu-Cl}. ESR X-band of polycrystalline **1** at 77, 300 K show axial spectra with the ratio A$_{77}$/A$_{300}$ = 4.51, and a linewidth increase by 14.5 % on going from 300 K to 77 K, suggesting a incipient ferromagnetic exchange interaction. ESR axial spectrum of **1** in solution shows abundant *hfs* and *shfc* interactions. Susceptibility *vs* Temperature data measured from 2-300 K range, show that the magnetic ordering may be due to Cu ions linking by oxygen bridges given place to a weak ferromagnetic interaction. The very weak exchange interaction, *J* = 0.103 cm^{-1}, is in agreement with the ESR spectra results and with a Cu^{II}—O...Cu^{II} direct interaction.

Introduction

In biological systems the presence of planar structures containing electron-donor atoms as nitrogen, oxygen, or sulfur atoms, which are capable of accepting an axial five-coordination have been of interest.[1-4] These systems are found in biological molecules and carry out important functions as photosynthesis,[5] reversible dioxygen linking,[6] electron transfer,[7] peroxidation,[8] among others. On the other hand, the benzimidazole moiety and some of its derivatives present in molecules as vitamin B_{12}[5] and Cu^{II}-benzimidazole complexes have been reported.[9,10] The benzimidazole group coordinated to transition metal ions, allows planarity to the structures, and combined with other important aminoacid ligands, produce complexes of interest, which can be copper biosites models.[1,4] In this work, we are reporting the synthesis, electronic studies and magnetostructural relations of a novel Cu^{II}- five-coordinated complex.

Results and Discussion

Crystal structure

Complex **1** crystallizes in an orthorhombic cell in the non-centrosymmetric space group $P2_12_12_1$ (Table 1), consistently with the chiral nature of the L-isoleucinate (L-Ile) ligand. The correctness of the absolute configuration for this ligand was confirmed by the refinement of a Flack parameter: x = -0.025(17) for 1310 Friedel pairs (64% of potential pairs have been measured). The asymmetric unit in the crystal contains one monomeric molecular complex [Cu^{II}(L)(L′)Cl] and one water lattice molecule. Ligands L and L' are 2-aminomethylbenzimidazole and L-isoleucinate, respectively (Figure 1a). Chelating behavior for both ligands correspond to common coordination modes, which were previously observed in other transition metal complexes, including Cu^{II} complexes. L-Ile coordinates through unprotonated amine function and one carboxylate O atom, as found for example in *trans*-bis(D,L-isoleucinato-*N,O*)-copper(II).[11] The conformation stabilized for L-Ile in **1** is slightly different from that observed in the free zwitterion,[12] allowing the amine group to coordinate to the metal centre: the torsion angle N12-C13-C14-O15 is 14.5(4)º in **1**, while free ligand is twisted by -19.0(2) and -41.4(2)º (two conformations are stabilized in the solid state). Ligand L adopts an almost planar conformation, common for this ligand, and coordinates through two N atoms in a chelating mode. Such a coordination has been described in a Cu^{II} complex including glycylglycinato as co-ligand,[13] and also in hexacoordinated Cu^{II} complexes.[14]

The trigonality index about Cu site in **1** is $\tau = 0.27$, close to the index expected for a square pyramidal environment, for which $\tau = 0$ ($\tau = 1$ for ideal trigonal bipyramidal geometry).[15,16] The equatorial plane containing N12, O15, N3 and N11 atoms is distorted, the r.m.s. deviation from a least-squares plane containing these atoms being 0.142 Å. Significantly different bond lengths are found, in the range 1.948(2)-2.015(3) Å (Table 2). The apical site is occupied by the chlorine atom, with a long Cu—Cl bond length (Table 2), characteristic of these structures.[17-20] The angle between the normal to the basal plane N12/O15/N3/N11 and the line Cu—Cl is 3.7°. These features suggest that the covalency of the O and N atoms towards Cu^{II} is very similar to each other (Table 2).

The molecules pack along the short cell axis [100], and the closest metal...metal separation is then $Cu…Cu^i = 5.7757(12)$ Å [symmetry code: (*i*) 1+*x*, *y*, *z*]. Other close intermolecular approaches in the solid state are Cu—Cl...Cl^{ii}—Cu^{ii} = 6.616(2) Å, Cu—O15...O15^i—Cu^i = 5.7757(12) Å, and Cu—O15...Cl^i—Cu^i = 6.088(3) Å [symmetry code: (*ii*) -1/2+*x*, 3/2-*y*, 1-*z*]. A potentially important close contact related to magnetic interactions is Cu—O15...Cu^i between two symmetry related molecules stacked along [100], with a O...Cu separation $R = 4.214(3)$ Å and a angle $\phi =$ Cu—O...Cu^i = 136.0(1)° > 90°.[9] Voids between complexes are filled by lattice water molecules, which are connected to complexes through rather weak hydrogen bonds involving amine NH_2 functional groups of both ligands *L* and *L'* as well as carboxylate O16 atom (see deposited CIF and Fig. 1b)

Table 1. Crystallographic data for **1**

Formula: $[C_{14}H_{21}ClCuN_4O_2]OH_2$	Fw = 394.35
$a = 5.7757(12)$ Å	cryst syst: orthorhombic
$b = 11.821(2)$ Å	space group: $P2_12_12_1$
$c = 25.244(3)$ Å	$D_{calc} = 1.520$ g.cm^{-3}
$V = 1723.5(5)$ Å^3	temp = 296(1) K
$Z = 4$, $Z' = 1$	$\lambda = 0.71073$ Å (Mo-$K\alpha$)
	$\mu = 1.441$ mm^{-1}
data used: 3351	parameters: 231
$R_1{}^a = 0.0347$ [2986 data with $F_0 > 4\sigma(F_0)$]	$wR_2{}^b = 0.0882$ [all data]

^{a} $R_1 = \dfrac{\sum \left| |F_o| - |F_c| \right|}{\sum |F_o|}$, $wR_2 = \sqrt{\dfrac{\sum w\left(F_o^2 - F_c^2\right)^2}{\sum w\left(F_o^2\right)^2}}$
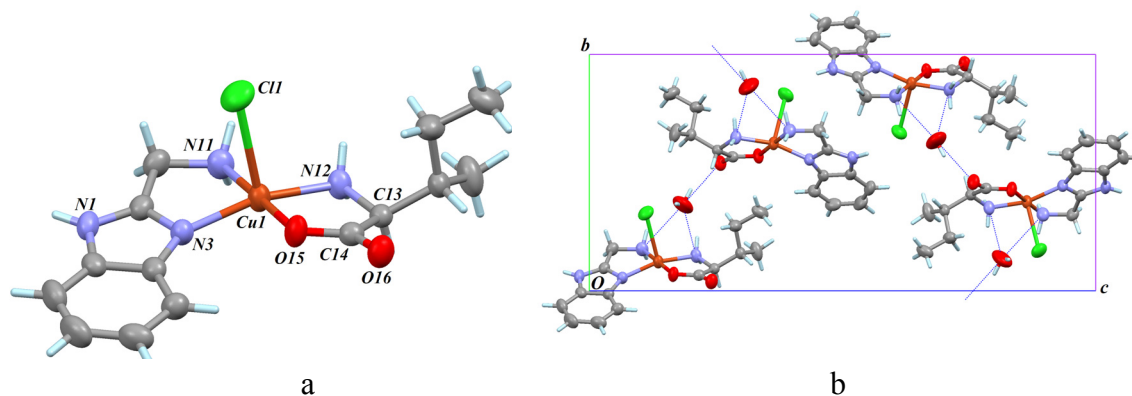
Figure 1. (a) Molecular structure of **1** with displacement ellipsoids drawn at the 50% probability level for non-H atoms. The water molecule has been omitted for clarity. (b) Crystal structure of **1** viewed down [100]. Dashed lines represent O...N contacts in hydrogen bonds involving the water lattice molecule.

UV/Vis and NIR spectroscopy

The UV/Vis/NIR spectrum of **1** shows π-π* transitions at 270 nm (ε = 126 M^{-1} cm^{-1}) and ligand-metal charge transfer transitions at 277 nm (ε = 129 M^{-1} cm^{-1}). At 603 nm with molar absorptivity of 9.41 M^{-1} cm^{-1} and oscillator strength of 1.93×10^{-3}, is observed a broad, asymmetric and short band, corresponding to d-d transitions characteristic of square pyramidal distorted structures of Cu^{II} compounds.[21-23] This band has been fitted to the combination of four Gaussian functions (Figure 2a). According with other experimental and theoretical results of Cu^{II}-compounds reported, the Gaussian functions number expected for square pyramidal structure, would be three, corresponding to $d_{x2-y2} \leftarrow d_{z2}$, $d_{x2-y2} \leftarrow d_{xy}$, $d_{x2-y2} \leftarrow d_{xz}$, d_{yz}, transitions.[24,25] We attribute the presence of the four Gaussian functions to the low symmetry in the first coordination sphere around of Cu^{II}, three nitrogen atoms, one chloro and one oxygen atoms. In addition, the chloro apical ligand shows a deviation of its perpendicularity to the square pyramidal base, which establish an interaction between electronic density of the chloro ligand and some of the atomic orbitals d_{xz} and d_{yz}, promoting a minimum differentiation (Figure 2 a, (a) and (b) bands) between both d atomic orbitals (Figure 2b).[24-26]

Table 2. Coordination bond lengths (Å) and angles (°) for **1**

Bond lengths			
Cu1-O15	1.948(2)	Cu1-N3	1.974(3)
Cu1-N12	1.976(3)	Cu1-N11	2.015(3)
Cu1-Cl1	2.6939(11)		
Bond angles			
O15-Cu1-N3	96.49(11)	O15-Cu1-N12	84.49(11)
N3-Cu1-N12	162.77(13)	O15-Cu1-N11	179.14(13)
N3-Cu1-N11	82.83(12)	N12-Cu1-N11	96.01(12)
O15-Cu1-Cl1	93.80(9)	N3-Cu1-Cl1	96.94(9)
N12-Cu1- Cl1	100.16(11)	N11-Cu1-Cl1	86.81(11)

IR spectrum of **1** shows a band at 3496 cm^{-1} characteristic of complexes with water of crystallization. At 3257 cm^{-1}, 2786 cm^{-1} and 2637 cm^{-1} the bands corresponding to the $\nu_{N—H}$ vibrations; at 3042 cm^{-1}, 2966 cm^{-1} the corresponding to $\nu_{C—H}$ aromatic vibrations; at 1616 cm^{-1} the $\nu_{C=O}$ vibration.[26-28] Far-infrared spectrum of **1** shows at 493 cm^{-1} and 404 cm^{-1} characteristic vibration $\nu_{Cu—N}$; at 446 cm^{-1} the $\nu_{Cu—O}$ vibration, at 302 cm^{-1} stretching vibration for $\nu_{Cu—Cl}$.[28-31] These IR data are in full agreement with the functional groups present in the structure.
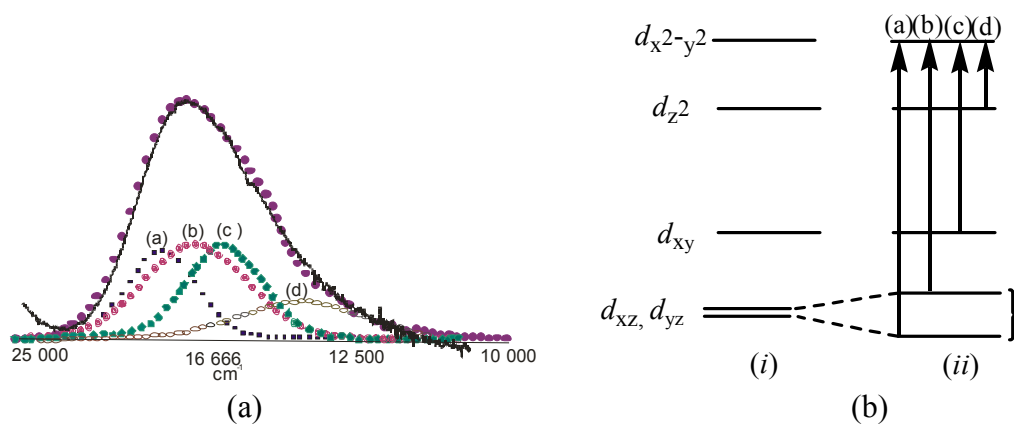

Figure 2. (a) Electronic spectrum in visible region of **1.** Experimental (—), adjusted by Gaussian curves and their sum (•••); (b) proposed *d-d* transitions in the low symmetry atomic *d* orbitals.

^{1}H NMR spectroscopy

^{1}H NMR spectrum of **1** is typical of paramagnetic compounds showing a collection of lines broadening in a 35 to 8 ppm range and other collection of sharp lines in a 6.5 to 1 ppm range.[32] It is clear to observe that both groups of chemical shifts show different relaxation times by dipolar relaxation of nearest ligand protons that are within a sphere of 4-5 Å radius from the metal, or contact relaxation to nearest neighbor ligand protons.[17, 21, 32-34] The assignment of the signals for

specific protons is not possible and less yet its quantified. The ^{13}C NMR experiment does not show any useful signal, because of the large noise/signal ratio.

ESR spectroscopy

ESR X-band spectra of the polycrystalline powdered sample of **1** were recorded at 25 different temperatures between 300 K and 77 K, and at 77 K in methanol solution with concentration varying from 10^{-2} M to 10^{-3} M. These samples do not show any additional resonances at zero field or any other field at any gain.
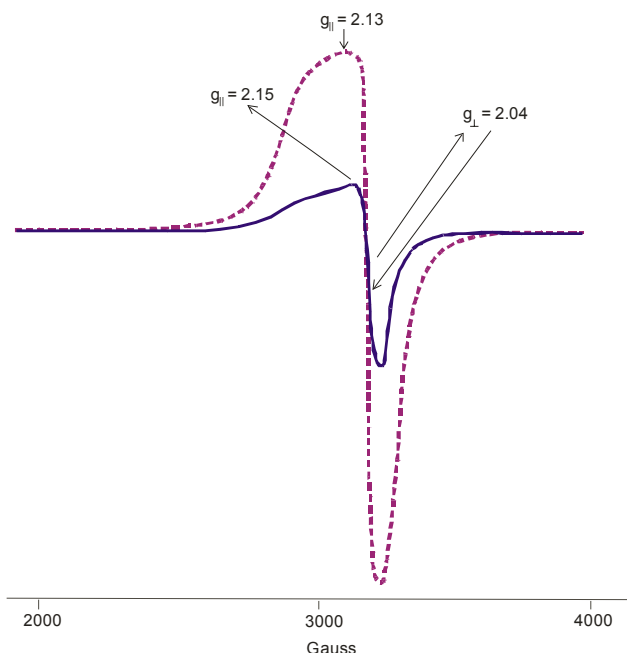

Figure 3. ESR spectra of powdered sample of **1** at 77 K (- - -) and 300 K (——).

At 300/77 K complex **1** powder sample exhibits axial singlet spectra,[21,34,35] with the magnetic parameters obtained from the simulations of the experimental ESR spectra using ES-PRIT computational program of Jeol.[36] The parameter values are $g_{\parallel}$ = 2.150/2.150, $g_{\perp}$ = 2.040/2.040 ($\bar{g}_{iso}$ value of 2.100), characteristic of $d_{x^2-y^2}$ ground state of unpaired electron and rhombic distortion.[37-41] The linewidth parameter is of 76.30G/88.9G (Figure 3). The area under the resonance absorption, A, increases by a factor of 4.51, and the linewidth, Γ, becomes 14% wider when the temperature is decreased from 300 K to 77 K spectrum. This ESR behavior of **1** is consistent with the presence of a weak ferromagnetic exchange interaction, in which the dipole-dipole interaction is still dominant.[42, 43]
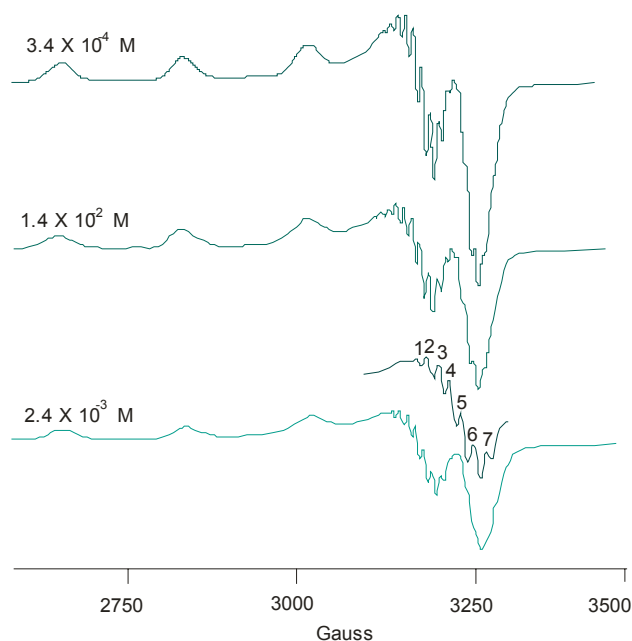
Figure 4. ESR spectra of **1** in solution at three different concentrations showing *hfs* and s*hfc* interactions. Only three different concentrations are considered for clarity in the spectra change.

ESR spectra of **1** in solution at six different concentrations in the range *ca* 3 mM to 0.2 mM (Figure 4), show hyperfine interactions splitting, *hfs*, with A_{hfs} value of *192* $\times$ 10^{-4} cm^{-1},[37] which is characteristic of normal tetragonal distorted Cu^{II}-complexes.[38,44,45] It is observed too a superhyperfine s*hfc* structure with A_{shfc} value of *9.24* $\times$ 10^{-5} cm^{-1}. The zoom on Figure 4 shows the ESR spectrum at the lowest concentration with seven superhyperfine splitting, corresponding to three first neighbors at Cu^{II} with $I_N = 1$. Note that the Γ values at all concentrations are identical, indicating that intermolecular dipolar interactions are not significant in this system, while intermolecular dipole-dipole interactions should be the main contribution to this width.[45]

Magnetic behavior

Molar magnetic susceptibility versus temperature, χ_M-T, of powder samples of **1** were measured in the temperature range from 2 to 300 K. Figures a shows χ_M-T plots fitted to eq (1) using a weak exchange interaction according to the Heisenberg model, with Hamiltonian, given by H_{ex} = -2J $S_1 \cdot S_2$, for a pair of exchange-coupled $S = 1/2$ spins: [46-48] Here the magnetization, M, is:

$$M = \frac{\left[Ng\beta \sinh\left(\frac{g\beta H}{kT} \right) \right]}{\left[\exp\left(-\frac{2J}{kT} \right) + 2\cosh\left(\frac{g\beta H}{kT} \right) + 1 \right]} \tag{1}$$

In Figure 5a the best fit is shown with solid line, where we used a exchange interaction about $J = 0.103$ cm^{-1}, g = 2.101, and $R^2 = 0.99875$.

The magnetic ordering could occur through the oxygen bridges linking the $Cu^{II}...Cu^{II}$ ions, as can be observed in the crystalline structure of **1,** shown in Scheme 1A, and it is through the coordinated O atom belonging to the carboxylate Cu—O...Cu. The distance O...Cu of 4.214(3) Å is one of the shortest between neighboring molecules, and accordingly, to Scheme 1A the magnetic exchange communication is through an zig-zag infinite chain. However, we must remark that other possible magnetic pathway may be through of Cu—O—C=O...H—N—Cu, which is through five atoms and with a O...H distance of 2.643 Å. This magnetic pathway is in a zig-zag infinite chain also (Scheme 1B). The results of the best fit, considering the Ising model, as shown (solid line) in Scheme 1 are: $J = 0.99$ cm^{-1}, g = 2.088, and $R^2 = 0.99903$ according to eq (2) (Figure 5b): [49]

$$\chi = \frac{\left(g^2 \mu_\beta{}^2 N\right)e^x}{\left[2kT\left(1+e^x\right)\right]}, \quad x = \frac{J}{kT} \tag{2}$$

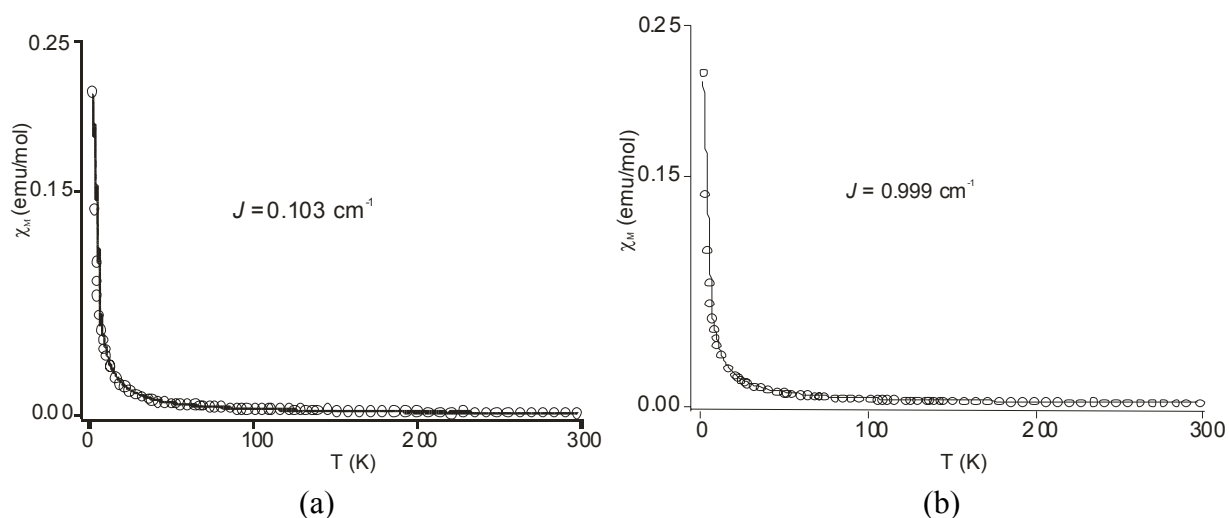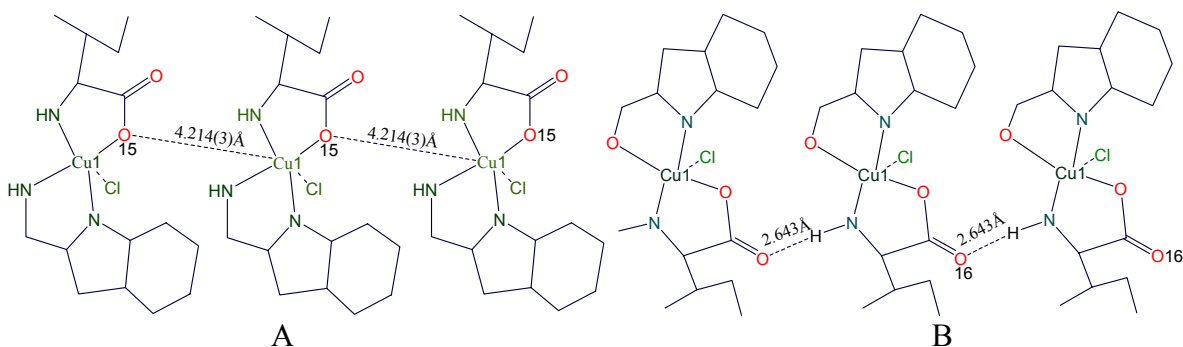(a)   (b)

Figure 5. Temperature dependence of χ_M *vs* T: (a) the experimental data open circles (ooo), solid line corresponds to the fitting using Myers expression, eq (1); (b) fit using Ising model.

A   B

Scheme 1

The fitting data using the Myers and the Ising models, for our magnetic measurements are in complete correspondence to ESR results too. The weak interaction is expected in function of the ratio areas and the width of the ESR spectra at 77 and 300 K. On the other hand, the low concentrations of **1** in solution that show *hfs* and *shfc* interactions informs that the ferromagnetic exchange interaction Cu-Cu must be weak. Different concentrations of **1** in solution show that the width line remains unchanged, that: a) dipolar interaction is more important than the exchange interaction, and b) meaning that this last interaction is very weak and direct, without linking bridges. Compound **1** obtained in this work resulted with an asymmetry to accept a fifth ligand in the apical position, giving rise to a local structure around the Cu^{II} ion which is typical of active sites of some Cu-proteins.

Experimental Section

General Procedures. Diffraction data for complex **1** were measured at room temperature on a Bruker P4 diffractometer (non-CCD detector) using standard procedures.[50] Data were corrected for absorption effects on the basis of 10 ψ-scans and the structure solved and refined using *SHELXTL*-Plus software.[51] A summary for data collection and refinement is given in Table 1, and details may be found in the archived CIF, along with complete geometric parameters.[52] All C-bonded H atoms were placed in idealized positions and constrained to ride on their carrier atom. N- and O-bonded H atoms were found in a difference map and refined with free coordinates. The geometry of the lattice water molecule was however regularized through soft restraints on distances: O—H = 0.85(2) and H...H = 1.41(2) Å.

The ^{1}H NMR spectra were recorded at 25 °C on a JEOL ECLIPSE 400 MHz spectrometer, using methanol-*d* solutions with ca 10^{-2} M in the 100 to -100 ppm range. ESR measurements were carried out on polycrystalline samples at X-band frequency (9.4 Ghz) on a Jeol JES-RES3X spectrometer, at 300 and 77 K with 100 KHz modulation frequency. At 77 K in methanol solutions (ca 10^{-2} M to 10^{-3} M) were recorded the ESR spectra. The g values were accurately determined by DPPH pitch. Magnetic measurements were carried out with a Quantum Design Magnetometer MPMS-5S, at 2000 Gauss, as applied field in the temperature range from 2-300 K, using gelatin capsule as the container of the samples. The elemental analysis (C, H) was carried out at USAI UANM Laboratories. Infrared spectrum of CsI pellet of the complex was recorded on a Nicolet Magna IR Spectrometer 750, at rt in the range 4000-200 cm^{-1}. Electronic spectrum was recorded on a Shimadzu spectrophotometer UV-3100 on ca 0.1×10^{-4} M, at rt, in methanolic solution in the range 190-1500 nm. Starting materials were purchased from Aldrich, Baker and Fermont laboratories.

Compound characterization. Compound **1** was obtained by García-Orozco method,[9] using optimized experimetal conditions. In a flask were placed 1.2 mmol of isoleucine with 0.9 mmol of aminomethylbenzimidazole hydrochloride, and 0.1 ml of hydrochloride acid solution 0.06

mM. The mixture was kept under magnetic stirring at rt during 5 min. After this time 1 mmol of $CuCO_3(OH)_2$ was added. The reaction mixture was kept under magnetic stirring for 30 min at rt. A blue solid is formed, filtered and crystallized from methanol/water. A blue crystal of the compound, suitable for X-ray diffraction (15 % yield, m.p. = 165-167 ^{o}C) was collected. Anal. Calc. for $C_{14}H_{23}ClCuN_4O_3$: C: 42.64, H: 5.88. Anal. Found: C, 41.65; H, 5.64. UV-Vis $\lambda_{max}/\varepsilon$ ($CHCl_3$) nm/mM^{-1}cm^{-1}: 270/126, 277/129, 603/9.41; IR ν_{max} (CsI) cm^{-1}: IR ν_{max} (CsI) cm^{-1}: 3257 cm^{-1}, 2786 cm^{-1} and 2637 cm^{-1} str N-H, 1616 str C=O, 493, 404 Cu-N, 446 Cu-O, 302 Cu-Cl; ^{1}H NMR (CD_3OD) ppm: 32.00, 25.24, 13.30, 10.46, 10.00, 6.30, 6.11, 5.48, 5.25, 4.62, 3.34, 3.30, 2.15, 1.49, 1.27, 1.17, 1.15; ESR: 300/77 (K) $g_{\parallel}$ = 2.15/2.15, $g_{\perp}$ = 2.04/2.04; A_{77}/A_{300}= 4.51, μ_{eff} = 1.90.

Acknowledgements

References and Notes

1. Sigel, H.; Martin, R. B. *Chem. Rev.* **1982**, *82*, 38.
2. Sanna, D.; Ágoston, S. G.; Sóvágo, I.; Micera, G. *Polyhedron* **2001**, *20*, 937.
3. Kozlevčar, B.; Glažar, L., Pirc, G.; Jagliči´c, Z.; Golobič, A.; Šegedin, P. *Polyhedron* **2007**, *26*, 11.
4. Adams, H.; Bailey, N. A.; Campbell, I. K.; Fenton, D. E.; He, Q.-Y. *J. Chem. Soc., Dalton Trans.* **1996**, 2233.
5. Stryer, L. *Biochemistry*, 3a. Ed., Freeman: USA, 1988.
6. Kendrew, J. C.; Dickerson, R. E.; Strandberg, B. E.; Hart, R. G.; Davies, D. R.; Phillips, D. C.; Shore, V. C. *Nature* **1960**, *185*, 422.
7. Gray, H. B.; Ellis, W. R. Jr. In *Bioinorganic Chemistry*, Bertini, I.; Gray, H. B.; Lippard, S. J.; Valentine, J. S., Ed., University Science Books: USA, 1994.
8. Saunders, B. C.; Holmes-Sidle, A. G.; *Peroxidase*, Butter Worths, USA, 1964.
9. 9, García-Orozco, I.; Tapia-Benavides, A. R.; Álvarez-Toledano, C.; Toscano, R. A.; Ramírez-Rosales, D.; Zamorano-Ulloa, R.; Reyes-Ortega, Y. *J. Mol. Struct.* **2002**, *604*, 57.
10. Riccardo F. C.; Williams, A. F.; Piguet, C. *Helv. Chim. Acta* **1998**, *81*, 548.
11. Martino, D. M.; Steren, C. A.; Calvo, R.; Piro, O. E. *J. Solid State Chem.* **1991**, *90*, 211.
12. Gorbitz, C. H.; Dalhus, B. *Acta Cryst.* **1996**, *C52*, 1464.
13. Liu, W.-L., Zou, Y.; Ni, C.-L.; Ni, Z.-P.; Li, Y-Z.; Yao, Y.-G.; Meng, Q.-J. *J. Coord. Chem.* **2004**, *57*, 899.

14. He, Y.; Kou, H-Z.; Wang, R-J.; Li, Y.; Xiong, M. *Transition Met. Chem.* **2003**, *28*, 464.

15. Addison, A. W.; Rao, T. N.; Reedijk, J.; van Rijn, J.; Verschoor, G. C. *J. Chem. Soc., Dalton Trans.* **1984**, 1349-.

16. Willett. R. D.; Pon, G.; Nagy, C. *Inorg. Chem.* **2001**, *40*, 4342.

17. Alcántara-Flores, J. L.; Vázquez-Bravo, J. J.; Gutiérrez-Pérez, R.; Ramírez-Rosales, D.; Bernès, S.; Ramírez Bokhimi, J. G.; Zamorano-Ulloa R.; Reyes-Ortega, Y. *J. Mol. Struct.* **2003**, *657*, 137.

18. Ayllón, J. A.; Santos, I. C.; Henriques, R. T.; Almeida, M.; Alcácer, L.; Duarte, M. T. *Inorg. Chem.*, **1996**, *35*, 168.

19. Fuji, Y.; Wang, Z.; Willett, R. D. *Inorg. Chem.*, **1995**, *34*, 2870.

20. Matsumoto, N.; Motoda, Y.; Matsuo, T.; Nakashima, T.; Re, N.; Dahan, F.; Tuchagues, J.-P. *Inorg. Chem.* **1999**, *38*, 1165.

21. Reyes-Ortega, Y.; Alcántara-Flores, J. L.; Hernández-Galindo, M. C.; Gutiérrez-Pérez, R.; Ramírez-Rosales, D.; Bernès, S.; Cabrera-Vivas, B. M.; Durán-Hernández, A.; Zamorano-Ulloa, R *J. Mol. Struct.* **2006**, *788*, 145.

22. Koolhaas, G. J. A. A.; Driessen, W. L.; Reedijk, J.; van der Plas, J. L.; de Graff, R. A. G. *Inorg. Chem.* **1996**, *35*, 1509.

23. Chavez, F. A.; Olmstead, M. M.; Mascharak, P. K. *Inorg. Chem.* **1996**, *35*, 1410.

24. Park, G.; Shao, J.; Lu, F. H.; Rogers, R. D.; Chasteen, N. D.; Brechbiel, M. W.; Planalp, R. P. *Inorg. Chem.* **2001**, *40*, 4167.

25. Duggan, M,; Ray, N.; Hathaway, B.; Tomlinson, G.; Brint, M. P.; Pelin, K. *J. Chem. Soc., Dalton Trans.* **1980**, 1342.

26. Ismail, K. Z.; El-Dissouky, A.; Shehada, A. Z. *Polyhedron* **1997**, *16*, 2909.

27. Nakanishi, K. *Infrared Spectroscopy Absorption*, 2nd Edn, Holden-Day: San Francisco, 1977.

28. Nakamoto, K. *Infrared, Raman Spectra of Inorganic and Coordination Compounds*, 4th Edn., Wiley: New York, 1986.

29. Boschmann, E.; Weinstock, L. M.; Carmack, M. *Inorg. Chem.* **1974**, *13*, 1297.

30. Papadopoulos, A. N.; Tangoulis, V.; Raptopoulou, C. P.; Terzis, A.; Kessissoglou, D. P. *Inorg. Chem.* **1996**, *35*, 559.

31. Choi, S-N.; Bereman, R. D.; Wasson, J. R. *J. Inorg. Nucl. Chem.* **1975**, *37*, 2087.

32. Bertini I., Ciurli S., Dikiy A., Gasanov R., Luchinat C., Martini G., Safarov N. *J. Am. Chem. Soc. 121*, **1999**, 2037.

33. Schneider H.-J, Londsorfer M., Weigand E. F. *Org. Magn. Reson. 8*, **1976**, 363.

34. Alcántara-Flores, J. L.; Ramírez-Rosales, D.; Bernès, S.; Pérez-Ramírez (Bokhimi), J. G.; Durán-Hernández, A.; Gutiérrez-Pérez, R.; Zamorano-Ulloa, R.; Reyes-Ortega, Y. *J. Mol. Struct.* **2004**, *693*, 125.

35. Mabbs, F. E.; Collison, D. *Electron Paramagnetic Resonance of d Transition Compounds*, Elsevier: Amsterdan, 1992.

36. Manual JEOL, ES-PRIT Series, ESR data system (System version 1.6), [4] Simulation, No. IER-PRIT-SIM-1 (ER630001-/631001-1), 1991**.**

37. Solomon, E. I.; Sundaram, U. M.; Machonkin, T. E. *Chem. Rev.* **1996**, *96*, 2563.
38. Bencini, A.; Bertini, I.; Gatteschi, D.; Scozzafava, A. *Inorg. Chem.* **1978**, *17*, 3194.
39. Rowland, J. M.; Olmstead, M. M.; Mascharak, P. K. *Inorg. Chem.* **2000**, *39*, 5326.
40. Bentiss, F.; Lagrenée, M.; Mentré, O.; Conflant, P.; Vezin, H., Wignacourt, J. P.; Holt, E. M. *Inorg. Chem.* **2004**, *43*, 1865.
41. Akhriff Y., Server-Carrió J., Sancho A., García-Lozano J., Escrivá E., Folgado J. V., Soto L. *Inorg. Chem.* **1999**, *38*, 1174.
42. Feher, G. *Electron Paramagnetic Resonance with Applications to Selected Problems in Biology*, Gordon and Breach, Science Publishers: New York, 1970.
43. Morrish, H. *The Physical Principles of Magnetism*, John Wiley: London, 1965.
44. Várnagy, K.; Szabó, J.; Sóvágó, I.; Malandrinos, G.; Hadjiliadis, N.; Sanna, D.; Micera, G. *J. Chem. Soc., Dalton Trans.* **2000**, 467.
45. Drago, R. S. *Physical Methods for Chemists*, 2a. Edn., Saunders College Publishing: EUA, 1992.
46. Marsh, W. E.; Patel, K. C.; Hatfield, W. E.; Hodgson, D. J. *Inorg. Chem.* **1983**, *22*, 511.
47. Myers, B. E.; Berger, L.; Friedberg, S. A. *J. Appl. Phys.* **1969**, *40*, 1149.
48. Hatfield, W. E.; Barnes, J. A.; Jeter, D. Y.; Whyman, R.; Jr. Jones, E. R. *J. Am. Chem. Soc.* **1970**, *92*, 4982.
49. Chandramouli, G. V. R.; Balagopalakrishna, C.; Rajasekharan M. V.; Manoharan, P. T. *Computers Chem.* **1996**, *20*, 353.
50. XSCAnS (release 2.21) Users Manual, Siemens Analytical X-ray Instruments Inc., Madison, WI, USA, 1996.
51. G. M. Sheldrick, SHELX97 Users Manual, University of Göttingen, Germany, 1997.
52. Atomic coordinates have been deposited with the Cambridge Crystallographic Data Centre. The coordinates can be obtained, on request from the Director, Cambridge Crystallographic Data Centre, 12 Union Road, Cambridge CB2 1EZ, UK. Deposition number: CCDC 646388.